Genetic and materials engineering to enhance inducible gene expression in lactobacilli

Marc Blanch-Asensio,[1,2], Varun Sai Tadimarri,[1,2], Roberto Martinez,[1], Gurvinder Singh Dahiya[3], Rahmi Lale,[3,4] and Shrikrishnan Sankaran[1]

[1] INM - Leibniz Institute for New Materials, Saarland University, Campus D2 2, 66123 Saarbrücken, Germany

[2] Saarland University, 66123 Saarbrücken, Germany

[3] Syngens AS, 7089 Norway

[4]Department of Biotechnology and Food Science, Faculty of Natural Sciences, Norwegian University of Science and Technology, Trondheim, N-7491 Norway

*E-mail: Shrikrishnan.sankaran@leibniz-inm.de

ABSTRACT

Lactiplantibacillus plantarum, a versatile member of the lactobacilli family, is widely recognized for its potential in healthcare, food production, and environmental biotechnology. Despite its inherent advantages and demonstrated potential as microbial chassis for biotechnological applications, its broader utility is constrained by a limited genetic toolbox, particularly the lack of robust inducible gene expression systems. Addressing this gap, we report the development of a novel inducible system for *L. plantarum* based on a strong bacteriophage-derived promoter and the food-grade inducer, cumate. This system demonstrates enhanced dynamic range and temporal control of gene expression while exhibiting interesting temperature and growth phase dependent phenomena that influence leakiness and induced expression levels. Interestingly, encapsulation of engineered *L. plantarum* strains in alginate-based hydrogels significantly reduces leaky expression and maintains induction efficacy. Our findings highlight the synergistic potential of combining genetic engineering with encapsulation strategies to enhance the functionality of recombinant lactobacilli. This engineered living material approach is promising for developing *L. plantarum* towards advanced applications in biotechnology, pharmaceutics, and living therapeutics.

Keywords: Engineered living materials, lactobacillus, cumate, inducible system, PEARL.

INTRODUCTION

Lactobacilli are highly valued for their diverse applications across healthcare, food production, and environmental remediation. Their suitability for specific "Generally Recognized as Safe" (GRAS) applications, tolerance to stress, and ability to thrive in various environments make them ideal candidates for probiotics, mucosal vaccines, and more (Rastogi and Singh 2022). Among their notable advantages is their use in fermented foods and their ability to modulate gut microbiota, lower cholesterol, and attenuate inflammatory diseases (Wang, Zhang et al. 2012), (Santos Rocha, Lakhdari et al. 2012). These characteristics highlight their potential as microbial chassis in diverse applications. Building on their inherent benefits, there has been growing interest in harnessing lactobacilli for advanced biotechnological applications with the highest number of reports based on the species *Lactiplantibacillus plantarum*. Genetically engineered lactobacilli have been explored as living therapeutics, oral vaccines, and drug delivery vehicles (Pan, Liu et al. 2021), (del Rio, Dattwyler Raymond et al. 2008), (Ortiz-Velez, Goodwin et al. 2020). For example, lactobacilli have been modified to produce recombinant proteins for pharmaceutical applications, including vaccines and mucosal therapeutics (Halbmayr, Mathiesen et al. 2008), (Scheppler, Vogel et al. 2002).(Pan, Liu et al. 2021)

However, the broader applicability of lactobacilli is hindered by their limited genetic toolbox. Unlike model organisms such as *E. coli*, lactobacilli lack robust genetic parts like strong promoters, effective repressors, and reliable inducible systems (Blanch-Asensio, Dey et al. 2024).This gap has slowed the development of advanced genetic circuits needed for more precise control of gene expression. In particular, reliable inducible gene expression systems have been particularly elusive to create. A few attempts have been reported like the xylose- or lactose-inducible systems but the fold changes on induction are relatively poor in these cases (<10x) (Heiss, Hörmann et al. 2016). The most reliable and widely used one is the pSIP system, based on the sakacin-inducible two-component system (Sørvig, Mathiesen et al. 2005), (Karlskås, Maudal et al. 2014), but is limited by reliance on a peptide inducer that is costly, prone to protease degradation, and sensitive to the bacterial growth phase. Inducible systems are vital for the genetic programmability of an organism since they allow temporal control over gene expression. In terms of recombinant protein production for biotechnology or pharmaceutic applications, this enables a separation between growth and production phases, which can enhance productivity and reduce metabolic burden. For living therapeutic or bioremediation applications, inducible systems act as genetic switches that enable biosensing functions or remote activation of desired responses like protein secretion. However, inducible gene expression in lactobacilli often suffer from challenges such as leaky expression or limited dynamic range.

Our recent studies have expanded the genetic programmability of *L.* plantarum (Dey, Blanch-Asensio et al. 2023). We developed a high-performance promoter-repressor system derived from bacteriophages with the potential to aid the development of inducible gene expression

(Blanch-Asensio, Tadimarri et al. 2024). Moreover, towards the applicability of such genetically engineered lactobacilli, we encapsulated them in core-shell alginate hydrogels to create the PEARL (Protein Eluting Alginate with Recombinant Lactobacilli) format (Tadimarri, Blanch-Asensio et al. 2024). These engineered living materials (ELM) provided benefits such as containment of the engineered bacteria, sustained protein release, and reduced metabolic toxicity for at least two weeks. It even stabilized the protein release profile compared to non-encapsulated bacterial cultures. These results suggested that the PEARL format enhanced the performance of engineered *L. plantarum* and is promising for further development.

Nevertheless, none of the previous reports achieved inducible gene expression with encapsulated *L. plantarum*. Thus, in this study, we introduce a novel inducible system for *L. plantarum* based on our previously reported strong promoter that responds to a food-grade molecule, cumate. We uncover interesting temperature and growth phase dependent phenomena that influence leakiness and induced expression levels. More interestingly, by encapsulating these engineered strains in an alginate-based hydrogel, we observed a sustained drop in leaky expression and maintenance of log-phase like expression levels. These interesting results suggest that this encapsulation strategy stabilizes inducible gene expression in *L. plantarum* and such an engineered living material (ELM) approach might be a promising for further development of responsive genetic parts in lactobacilli.

EXPERIMENTAL SECTION

Strains, media and plasmid vector

L. plantarum WCFS1 was used in this study. The strain was grown in De Man, Rogosa and Sharpe (MRS) media (Carl Roth GmbH, Germany, art. no. X924.1). The strain was grown at either 30° or 37 °C (it is indicated in each case), and 250 revolutions per minute (rpm). The media of the engineered strains were supplemented with 10 µL/mL of erythromycin (Carl Roth GmbH, Germany, art. no. 4166.2). For the cloning of most of the plasmids, NEB DH5-α competent *E. coli* cells were used (New England Biolabs GmbH, Germany,Art. No. C2987). Engineered *E. coli* was grown in Luria-Bertani (LB) medium (Carl Roth GmbH, Art. No. X968.1) supplemented with 200 µg/mL of erythromycin at 37 °C and 250 rpm shaking conditions. The pLp_3050sNuc plasmid (Addgene plasmid # 122030) was the backbone vector for all the plasmids used in this work.

Molecular cloning reagents

Primers were synthesized by Eurofins Genomics GmbH (Köln, Germany). All the primers used in this study are listed in **Table S1**. Synthetic gene fragments were ordered as eBlocks from Integrated DNA Technologies (IDT) (Coralville, USA). The codon

optimization tool of IDT was used to codon-optimize the eBlocks (selecting the option for *Lactobacillus acidophilus*). All the eBlocks used in this study are listed in **Table S2**. For the polymerase chain reaction (PCR), Q5 High Fidelity 2X Master Mix (NEB GmbH, Germany, No. M0492S) was used. 1 kb Plus DNA Ladder (Catalog Number 10787018) was purchased from ThermoFisher Scientific (Germany) and used as reference in gel electrophoresis. The Wizard® SV Gel and PCR Clean-Up System (Promega GmbH, Germany, Art. No. A9282) was used to purify the PCR products. DNA assembly was performed using the HiFi Assembly Master Mix (NEB GmbH, Germany, Art. No. E5520S). The Qiagen GmbH (Hilden, Germany) plasmid extraction kit was used to lyse and extract the plasmids from E. coli DH5α. The Quick Blunting Kit (NEB GmbH, Germany, Art. No. E1201S) and the T4 DNA Ligase enzyme (NEB GmbH, Germany, Art. No. M0318S) were used for circularizing the purified PCR products.

Plasmid construction

The eBlocks were designed with compatible ends (20 base-pair overhangs) to the backbone vector. Each eBlock was resuspended with 20 µL of previously autoclaved MQ water and used directly in the HiFi assembly reaction following the manufacturer's protocol. Right after, the assembled products were transformed into NEB DH5-α competent *E. coli* cells following the manufacturer's heat shock protocol. Plasmids were extracted from *E. coli* DH5-α cells and used for transforming *L. plantarum* WCFS1 after sequence verification by Sanger sequencing (Eurofins Genomics GmbH (Köln, Germany)). All eBlock sequences are shown in **Figure S0**.

***L. plantarum* WCFS1 competent cell preparation and DNA transformation**

Prior to electroporation, *L. plantarum* WCSF1 competent cells were prepared as described in (Blanch-Asensio, Dey et al. 2023). DNA transformation was done by electroporation, following the procedure described in (Blanch-Asensio, Dey et al. 2023).

Gene expression system induction

Vanillic acid and 4-isopropylbenzoic acid were purchased at Sigma Aldrich (Catalog number H36001 and 268402, respectively). Anhydrotetracycline was purchased at Cayman Chemical (Item no. 10009542). All inducers were resuspended in pure ethanol. The concentrations used for inductions were: 50 µM of vanillic acid for the vanillate system, 200 nM of aTc for the aTc system, and 0.1 to 100 µM (indicated in each experiment) of 4-isopropylbenzoic acid for the cumate system. The induction time is

indicated in each experiment. The pSIP system induction was done using the SppIP peptide (GeneCust, Boyes, France), to a final concentration of 25 ng/mL.

Flow cytometry analysis

Engineered *L. plantarum* WCSF1 were grown in 4 mL of MRS media supplemented with 10 µg/mL erythromycin at 37 °C and 250 rpm. The next day, bacteria were sub-cultured to an OD_{600} of 0.01 in 2 mL of MRS media supplemented with 10 µg/mL erythromycin and grown at 37 °C with shaking (250 rpm) for a period of 8 h. For the induced conditions, the inducers were added along with the erythromycin. After that, 1 mL of the bacterial cultures were pelleted down by centrifugation at 6000 rpm for 2 minutes. The supernatant was discarded carefully, and the pellets were resuspended in 1 mL of sterile Dulbecco's 1X PBS (DPBS). Finally, the mixtures were serially diluted by a 10^4 Dilution Factor, and 5,000 bacterial events were recorded for analysis using Guava easyCyte BG flow-cytometer (Luminex, USA). The fluorescence intensity of mCherry was measured using excitation by a green laser at 532 nm (100 mW) and the Orange-G detection channel 620/52 nm filter was used for signal analysis. The Luminex GuavaSoft 4.0 software for EasyCyte was used for the analysis and representation of data.

Microplate reader setup for induction levels assessment

Engineered *L. plantarum* WCSF1 were grown and sub-cultured following the same procedure as for the flow cytometry analysis. Here, bacteria were grown and induced for a period of 5 to 8 hours (the exact time and cumate concentration are indicated in the results section). Once the bacterial pellets were resuspended in 1 mL of DPBS, 200 µL of the mixture were transferred to a UV STAR Flat Bottom 96 well microtiter plate (Greiner BioOne GmbH, Germany). The Microplate Reader Infinite 200 Pro (Tecan Deutschland GmbH, Germany) was used to quantify the levels of fluorescence. The mCherry fluorescence intensity was measured using the excitation/emission values: Ex_{λ} / Em_{λ} = 587 nm/625 nm. The fluorescence values were normalized with the OD_{600} of the mixtures (quantified by measuring the absorbance at 600 nm) to calculate the Relative Fluorescence Units (RFU) (Fluorescence/OD_{600}). In all cases, the Z-position was set at 19000 µm, the gain settings at 80-100 (indicated in the results section), and the readings were taken from the top.

Microplate reader kinetics setup for induction assessment

Engineered *L. plantarum* WCSF1 were grown and sub-cultured following the same procedure as for the flow cytometry analysis. After 8 hours of growth, bacteria were again diluted to an OD_{600} of 0.01. Next, bacteria were induced and transferred to a 96-well plate

(200 µL per well). The same parameters/measurement were taken every 30 minutes for 10 to 16 hours (indicated in the results section). RFU values were calculated as described in the previous section.

Macro-PEARL fabrication and cumate-responsiveness

Fabrication

3 wt% alginate solution was prepared by dissolving alginate in sterile MilliQ water, followed by autoclaving it for 15 minutes at 121 °C. Equal amounts of 3 wt% alginate and *L. plantarum* resuspended in LB medium (approximately 10^8 cells per mL) were mixed and vortexed to obtain the core solution (of 1.5 wt%). Equal amounts of 3 wt% alginate and sterile MQ water were mixed to obtain the shell solution (of 1.5 wt%). 10 µL droplets of core solution was pipetted and dropped into a 5 wt% CaCl2 solution (Ionic crosslinker). The droplets were left to polymerize in ionic crosslinker for 15 minutes, core beads were collected and washed thrice with sterile MQ water. Alginate core beads were dipped into an eppendorf with 1.5 wt% shell alginate solution and core bead with 25 µL of shell solution was pipetted and dropped into 5 wt% cross-linker solution. Core-shell alginate beads were left to polymerize in the cross-linker solution for 15 minutes before induction.

Cumate induction

PEARLs were transferred a 96-well plate, and 200 µL of LB media with or without cumate were added. Next, the micro-plate reader was used to track any bacterial leakiness (bacterial growth as an increase in absorbance at 600 nm), and mCherry production (Ex/Em = 587/625 nm) for 24 to 70 hours depending on the experiments. Manual gain was set at 100, Z-position at 19000 µm and integration time was 20 µs.

Micro-PEARL fabrication, secretion assessment and cumate responsivness

Fabrication

Core and shell solution were prepared in the same compositions as prepared for macropearls. 5 mL of core solution was filled in a 5 mL syringe and 20 mL of shell solution was filled in a 20 mL syringe. Microbeads were fabricated using encapsulator B-390 (Buchi, Switzerland). Autoclaved reaction vessel was arranged with 150 µm nozzle (for core) and 300 µm nozzle (for shell). Syringes with core and shell alginate solutions were secured to the respective entry points of aseptic reaction vessel. 200 mL of crosslinker solution (5 wt% CaCl2 solution) was introduced into the reaction vessel through the hose with filter (Sartorius, Germany). Encapsulator device was switched on and voltage (1600 V), frequency (910 Hz), syringe pump for core (20 milliliter/second), syringe pump for shell (7

milliliter/second) and stirrer (40 %) were enabled. The microbeads with core and shell flow drop into the reaction vessel until the core solution is syringe runs out. Microbeads were left in the reaction vessel for upto 15 minutes for polymerization. Microbeads were collected in a sterile schott flask connected to the device, through an efflux port at the bottom of reaction vessel. Reaction vessel and nozzles were cleaned by pumping with sterile water and the device was autoclaved.

NucA secretion assessment

After three washes with sterile MQ water, the micro-PEARLs were collected with a sterile spatula and placed in the center of DNase agar (Altmann Analytik GmbH, Germany) plates supplemented with 10 µg/mL of erythromycin and incubated at 37°C for 24 h. The next day, the discoloration zone was captured using the BioRad Gel Documentation System.

Cumate induction

After three washes with sterile MQ water, the micro-PEARLs were collected with a sterile spatula and placed in either 2-mL tubes or a 12-well plate. For the induction in the tubes, 1 ml of LB media with cumate was added. For induction in the plates, 500 µL of LB with cumate was added per well. Induction was performed for 24 hours. After that, induction was assessed with BioRad Gel Documentation System or the Keyence microscope (BZ-X800E).

Fluorescence Microscopy

The Keyence microscope (BZ-X800E) was used to perform microscopy of micro-PEARLs. After the induction, micro-PEARLs were transferred to a 12-well plate with glass bottom for better imaging. Multichannel images of micro-PEARLs were captured in 4x and 10x (S plan fluor objective) magnification using the CH3 (red fluorescence) and CH4 (brightfield) channels. The images were processed and analysed using ImageJ.

Statistical analysis

Statistical analysis was done using GraphPad Prism 7.0 software. Student's T-tests were used to determine statistically significant differences among the means of the groups. The differences among groups are indicated as: no statistically significant difference (ns), *p*-values <0.05 (*), *p*-values <0.01 (**), *p*-values <0.005 (***), *p*-values <0.001 (****).

RESULTS AND DISCUSSION

1) Inducible gene expression systems

In this study, we aimed to convert the strong constitute promoter P_{tec} into one that is inducible. For that, we engineered the promoter to make it responsive to three single-component inducible systems that have previously shown promising results in other bacteria. We selected the anhydrotetracycline (aTc) inducible system, proven to work in multiple bacteria such as *Escherichia coli*, *Vibrio cholerae* or *Streptococcus suis (Lutz and Bujard 1997)* (Bina, Wong et al. 2014) (Zhang, Zou et al. 2022), the cumate inducible system, which worked well in *Pseudomonas aeruginosa* and *Bacillus* subtilis (Klotz, Kaczmarczyk et al. 2023), (Seo and Schmidt-Dannert 2019) , and the vanillate inducible system, which showed promising results in *E.* coli (Kunjapur and Prather 2019). To reversibly repress the activity of P_{tec}, we flanked the promoter by the corresponding operators, one placed upstream and the other downstream of the promoter sequence (**Figure S1A**).

All three systems were designed with the same plasmid architecture, which harbored the P_{256} origin of replication and erythromycin resistance gene. An mCherry reporter gene was encoded downstream of the operated P_{tec} promoter, and each inducible-system's repressor (tetR, cymR and vanR) was driven by a moderate strength constitutive promoter, P_{23} (**Figure 1A**). In this way, the repressor gene would always be ON, whereas the inducible gene, mCherry, could be turned ON and OFF upon addition of the given inducer (aTc, cumate and vanillate) (**Figure 1B**).

Using flow cytometry, we assessed the responsiveness of each system to the given inducer after 8 hours of induction, seeking a system that shows strong P_{tec} repression in the absence of the inducer and prominent expression levels after induction. The aTc system showed very little levels of leakiness without the addition of inducer but poor levels of expression upon induction with 200 nM of aTc. The cumate system was more promising, with low levels of leakiness when uninduced and signficantly higher levels of mCherry expression upon induction with 100 µM of cumate. Finally, the vanillate system showed high levels of leakiness when uninduced and only slightly higher levels of expression with 50 µM vanillate (**Figure 1C**). We confirmed these results by fluorescence intensity measurements and quantified expression levels for each system after 5 hours of induction. These results confirmed that the system with the best induction was the cumate system, with a 27-fold change increase in mCherry expression after induction. The fold-changes were 3x and 2x for the aTc and vanillate systems, respectively. (**Figure S1B**). Overall, all three systems were responsive to their inducers, but since the cumate system offered the best performance, we proceeded to further characterize and optimize this system.

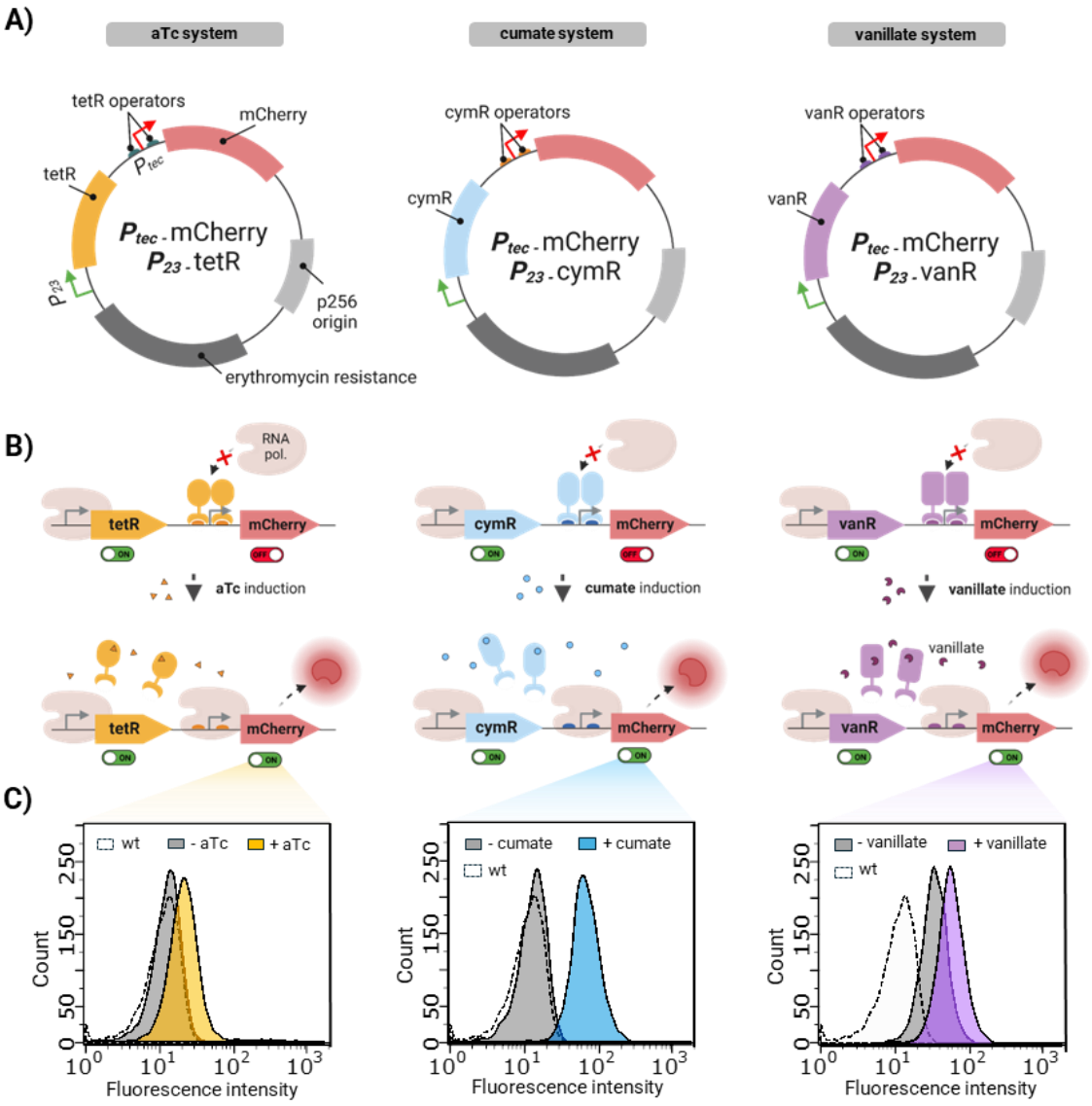

Figure 1: *Inducible gene expression systems adapted for L. plantarum*. **A)** Plasmid maps for the aTc, cumate and vanillate systems depicting all the relevant genetic parts. **B)** Schemes showing the mode of action of the three inducible systems, and the expected outcome after addition of the inducers. **C)** Histograms obtained by flow cytometry showing the red fluorescence intensity of the uninduced and induced states of each system. For all, the fluorescence intensity of non-engineered *L. plantarum* is shown as reference for leakiness. Bacteria were subcultured to an OD_{600} of 0.05 and induced for 8 hours with 200 ng of aTc, 100 µM of cumate and 50 µM of vanillate, respectively.

2) Characterization of the cumate inducible system

First, we tested whether the inducible system responds to cumate only due to inhibition of the CymR repressor. Hence, in the cumate inducible plasmid, we removed the P_{23}_cymR gene and observed that bacteria constitutively produced as much mCherry as the variants with the repressor that were induced with cumate (100 µM). This not only proved that induction was mediated purely through the repressor but also suggested that cumate fully inactivated it. (**Figure 2A**). By varying the inducer concentration, we further determined that 5 µM cumate was sufficient for maximal induction below which expression levels dropped in a seemingly linear manner below 1 µM. This suggested the possibility to tune expression levels by varying the concentration of cumate in the culture. (**Figure 1B**).

Nevertheless, we observed considerable leakiness in the system, indicating that repression of the inducible gene is incomplete in the absence of the inducer. We evaluated the leakiness of the system by tracking the increase in fluorescence without the inducer for 10 hours with P_{23}_cymR cultures having different starting bacterial densities - OD_{600} of 0.3, 0.1 and 0.01. We noticed a correlation between the bacteria growth and the leakiness of the system since fluorescence detection was delayed for 0.01-OD_{600} bacteria (**Figure 2C**). Next, we repeated the kinetics at OD_{600} of 0.01, but inducing the bacteria with 5 µM of cumate. We could start detecting mCherry expression approximately 3 hours after induction, whereas the detection was pushed after 7 hours without inducer (**Figure S2A**).

These results proved that it is possible to regulate the expression of the strong constitute promoter P_{tec} in an inducible manner. Nevertheless, the system leaks after a certain amount of time. We speculated that the leakiness could be associated with insufficient expression of the CymR repressor driven by the P_{23} promoter. Hence, we developed two additional variants by replacing P_{23} for a P_{tlpA}, a stronger constitutive promoter (P_{tlpA}_cymR variant), and by the natural (non-operated) P_{tec} promoter (P_{tec}_cymR variant) (**Figure S2B**).Unfortunately, we observed similar trends as with the P_{23}_cymR variant, with leakiness in the repression of P_{tec} after 6-8 hours of growth (**Figure S2C-D**).

Since swapping the promoter did not address the leakiness problem, we designed a different genetic architecture for the cumate system with a feedback loop. We cloned both genes, cymR and mCherry, under the operated P_{tec} promoter. Thus, both genes are regulated by the same promoter region, which should only be fully active in the presence of cumate (**Figure S3A**). To ensure production of both proteins, we included P_{23} ribosome-binding site between the STOP codon of the mCherry and the START codon of the cymR gene (**Figure S3B**). We termed this variant P_{tec}_cymR_P (polycistronic). This variant showed similar results

concerning the leakiness of the system, however, interestingly the overall levels of production were higher (**Figure S3C**).

Furthermore, through kinetic studies, we could calculate the fold-changes between the uninduced and induced states for all the variants and determine when each variant starts leaking. We observed that the variant that showed higher fold-change was the initial P_{23}_cymR variant, with a 65-fold change after 6 hours of induction (**Figure S3D**). The P_{tlpA}_cymR variant showed a 23-fold change after 6.5 hours. The P_{tec}_cymR variant showed a 13-fold change after 8 hours. Finally, the P_{tec}_cymR_P exhibited a ~9-fold change after 6 hours (**Figure S3D**). We decided to continue the characterization of the system by performing further experiments with the with P_{23}_cymR and the P_{tec}_cymR_P variants, since the former showed better fold-changes and the latter higher overall production.

Next, we compared the induction of these two variants with the most widely used inducible system in *L. plantarum*, the pSIP system. For that, we cloned the same reporter mCherry gene in the pSIP series 403 and 409. For proper comparison, we grew the bacteria to three different OD_{600} and performed the induction with either cumate for the P_{23}_cymR and the P_{tec}_cymR_P variants, or the inducing peptide SppIP for the pSIP-carrying bacteria. We could observe clear differences between the cumate and the pSIP systems. Firstly, the pSIP systems seemed not to leak at any of the assessed OD_{600}-inductions. Nevertheless, the overall levels of expression were significantly lower compared to the cumate systems (**Figure 3D, Figure S4**). For instance, after 12 hours of induction, the production of the pSIP_409 system (higher production than pSIP_403), was 8 to 17 times lower than the cumate systems across the different OD_{600}-inductions (**Figure 3D**).

Altogether, these results showed that it is possible to maintain the strong constitutive promoter P_{tec} inactive during the early and mid-log phase of growth. Yet, finding a method to decrease the leakiness of the cumate system and increase the uninduced-induced states fold-change would add great value to the genetic programmability of *L. plantarum*.

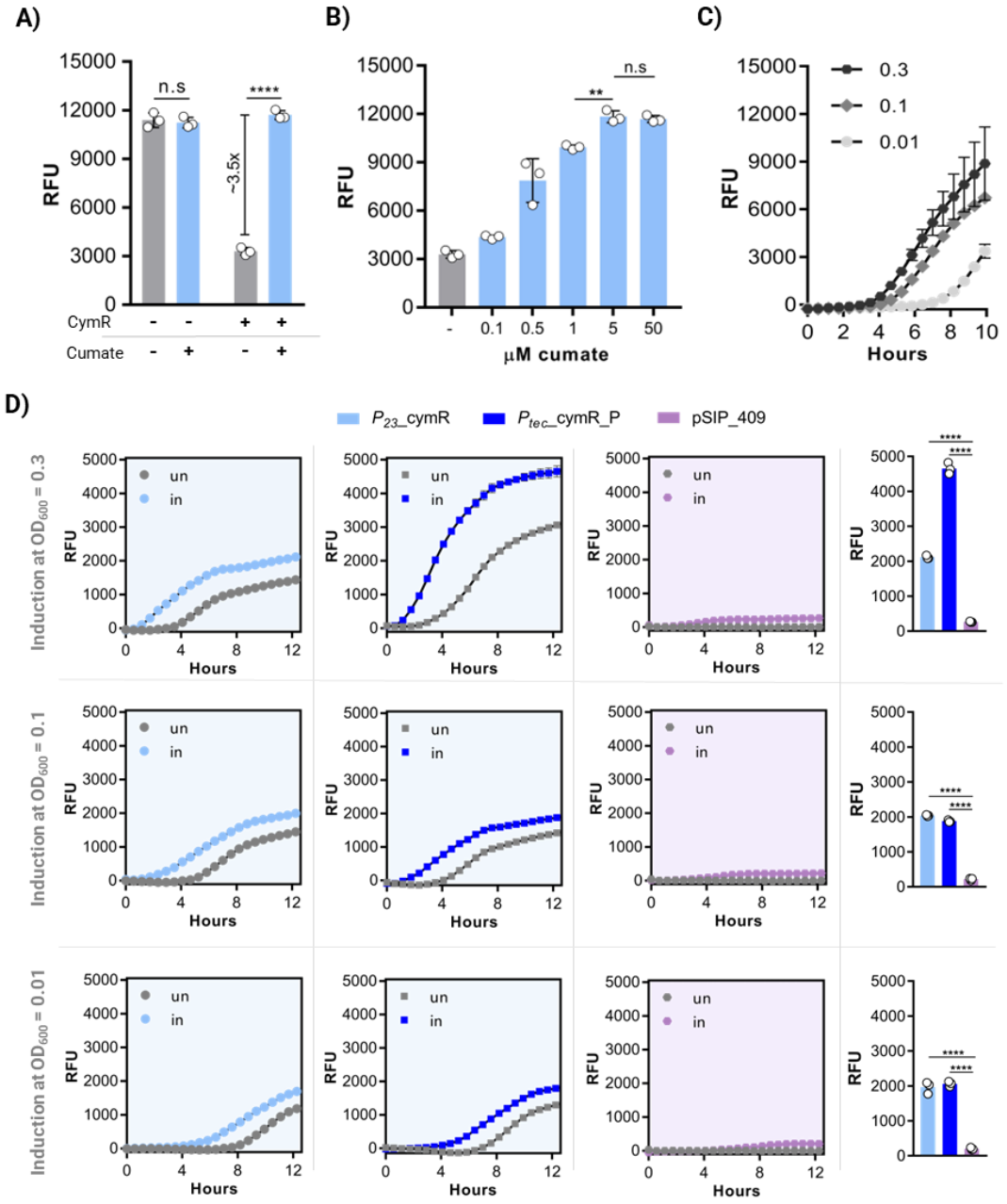

Figure 2*: Characterization of the cumate inducible system*. **A)** RFU values after 8-h induction with 100 µM of cumate. When the CymR is not encoded in the plasmid (-), when CymR is encoded in the plasmid (+). When cumate is not added in the media (-). When cumate is added to the media (+). no . **B)** RFU after inducing with different cumate concentrations for 8 hours. . **C)** Effect of the sub-culturing in the leakiness of the cumate system. **D)** Comparison between the P_{23}_cymR, P_{tec}_cymR_P, and pSIP_409 variants. Bacteria were induced at three different OD_{600} with 5 µM of cumate. Same induction for the pSIP_409 variant. The bar graphs on the right show the overall expression after 12 hours for all the three inducible systems. Values in the plots are the means and SD, N=3.

3) Double induction for maximized response

We theorized that temperature could be one factor influencing the leakiness of the cumate system since *L. plantarum* grows faster at temperatures around 37 °C and we have previous knowledge about higher promoter activity in *L. plantarum* at elevated temperatures (Dey et al. 2023). Hence, we decided to study the thermo-responsiveness of the P_{tec} promoter, and we observed that this promoter is two-fold stronger at 37°C compared to 30°C. This finding suggested that we could play around with the temperature in the induction of the cumate system. We therefore came up with the concept of "*double induction*", involving both temperature and cumate as inducers of the same system (**Figure 3B**). We speculated that growing bacteria at 30°C would keep the inducible gene shut down (OFF state) due to both the lower activity of P_{tec} at 30°C and the repression by cymR. On the other hand, growing the bacteria at 37°C and in the presence of cumate would allow high levels of gene expression (ON state).

We first evaluated the double induction through flow cytometry for the P_{23}_cymR variant. Cultures prepared at OD_{600} of 0.01 were induced with 5 µM of cumate and incubated at both 30 and 37 °C for 8 hours. Results showed low leakiness of the system at 30°C without induction, and prominent levels of mCherry expression at 37°C (**Figure 3C**). Besides, induction at 30°C also worked very efficiently, with the whole population switching to higher levels of fluorescence intensity. The double induction could even be visually noticeable in the bacterial pellets (**Figure 3C**), with an increase in pink color with both temperature and induction.

After these promising results, we were interested in estimating the fold-change differences in the double induction. For that, we used the microplate reader to accurately track mCherry expression over time. The P_{23}_cymR variant exhibited a considerable delay in the system leakiness when grown at 30 °C instead of 37°C while maintaining notable induced expression in the presence of cumate (**Figure 3D**). At 10 h, we calculated an 80-fold difference between uninduced and induced states at 30°C, and a 100-fold difference between the uninduced state at 30°C and induced state at 37°C (**Figure 3E**). We also evaluated the double induction response for the P_{tec}_cymR_P variant since it was able to achieve higher levels of overall production. We could detect a similar response, a prominent delay in the leakiness when bacteria were grown at 30°C (**Figure 3F**). For this variant, we estimated a cumate-driven 72-fold increase in expression at 30°C, and a remarkable 215-fold increase in expression at 37°C with cumate compared to 30°C without cumate after 10 hours of growth.

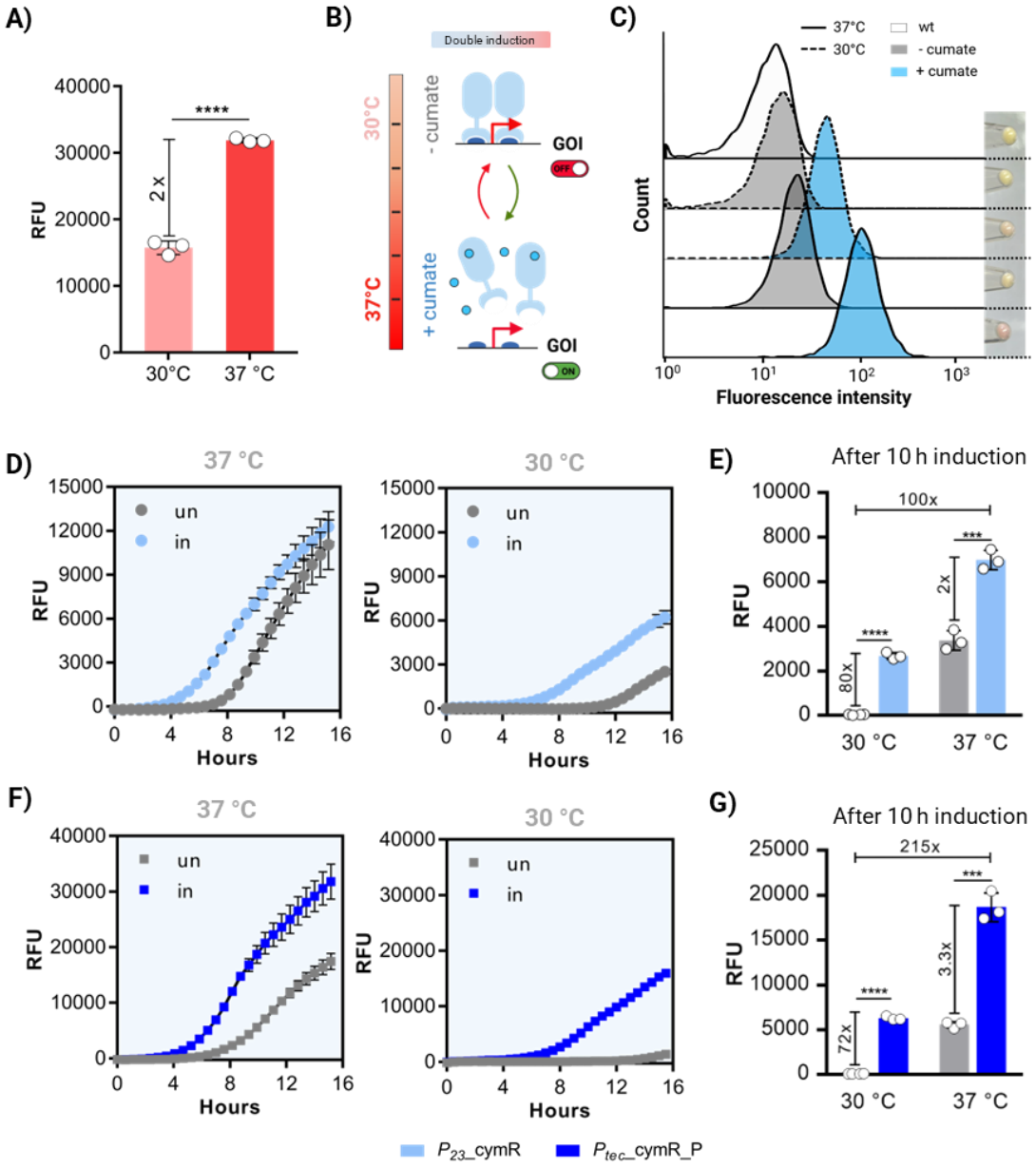

Figure 3: *Double induction approach involving temperature and cumate*. **A)** Thermo-responsiveness in terms of RFU for the P_{tec} promoter when grown at 30 and 37°C. **B)** Double induction scheme involving both temperature and cumate. Proper turning on of the gene is achieved via both the incubation at 37°C and addition of cumate. **C)** Histograms showing the fluorescence intensity (after 8 hours) of the P_{23}_cymR variant at 30 and 37°and with and without addition of cumate. Bacterial pellets are shown on the right of each condition. **D)** RFU values of the P_{23}_cymR variant when induced at 37°C and 30°C for 16 hours. **E**) RFU values corresponding to hour 10 after induction for the P_{23}_cymR variant when induced at 37°C and 30°C. **F**) RFU values of the P_{tec}_cymR_P variant when induced at 37°C and 30°C for 16 hours. **G**) RFU values corresponding to hour 10 after induction for the P_{tec}_cymR_P variant when induced at 37°C and 30°C. Values in the plots are the means and SD, N=3.

Based on these results, we hypothesized that the double induction approach could be used to clone challenging genes into *L. plantarum* for strong expression with P_{tec}. In previous work, we have experienced that *L. plantarum* can introduce mutations in genes when P_{tec} is used to produce a complex protein, probably due to high levels of protein production that end up being toxic or supposing a metabolic burden to bacteria (Tadimarri, Blanch-Asensio et al. 2024). For example, the elafin protein could never be cloned under P_{tec}.

4) Cumate inducible system in PEARLs

Next, we assessed the performance of the cumate system when bacteria are encapsulated within materials as an ELM format. Given the promising results with constitutive expression when encapsulating *L. plantarum* in alginate beads (PEARLs), we opted for employing this encapsulation method first. We speculated that the cumate inducer would be able to diffuse inside the beads thus activating the mCherry gene expression of the contained bacteria **(Figure 4A**).After fabricating the alginate beads for the P_{23}_cymR and the P_{tec}_cymR_P variants, we induced them by adding cumate to the media surrounding the beads in a 96-well and measured fluorescence over 24 hours. For the P_{23}_cymR variant, the induced beads started showing mCherry production after 4 hours of growth, and the overall fluorescence kept increasing over 24 hours (**Figure 4B**). The non-induced beads only showed low levels of leaky mCherry production after 16 hours (**Figure 4B**). These results suggest that encapsulation is useful to contain the leakiness of the cumate system, probably by limiting bacterial growth. On the other hand, the induced production levels of the P_{tec}_cymR_P variant were slightly higher than the P_{23}_cymR variant, yet, the non-induced beads also showed higher levels of leakiness after 15 hours (**Figure 4C**). We also evaluated the induction levels of the pSIP_409 system in alginate beads. The induction worked but the production levels were ~37 and ~50 times lower than the P_{23}_cymR and the P_{tec}_cymR_P variants, respectively (**Figure S5**).

After these results, we wanted to assess whether the non-induced P_{23}_cymR-based beads would leak after longer incubation time Hence, we monitored mCherry expression over 70 hours and observed that the system leaked after roughly 15 hours, but the mCherry level only plateaued after that. For the induced beads, the mCherry production started dropping after 23.5 hours, suggesting a saturation of the expressed protein within the bacteria and slowdown in its activity (**Figure 4D**). On estimation of the fold-change between the induced and uninduced conditions, the biggest difference was after 10.5 hours of incubation, and after 24 hours it stabilized within 25x-35x (**Figure 4E**).

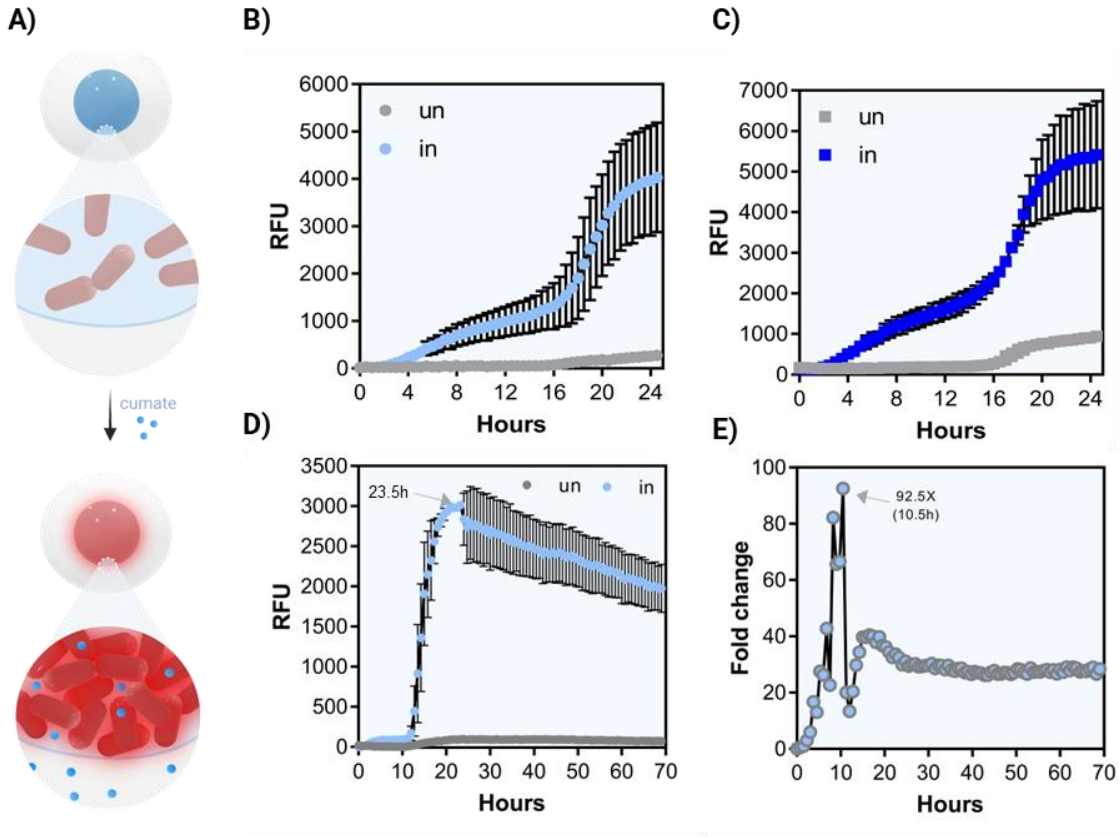

Figure 4: *Cumate inducible system in alginate beads*. **A)** Scheme showing the induction of L. *plantarum* bacteria harboring the cumate system when encapsulated in alginate beads. Upon induction, the core of the beads turns red due to bacterial activation and subsequent mCherry intracellular production. **B)** RFU values of P_{23}_cymR-based alginate beads after induction with cumate for 24 hours. **C)** RFU values of P_{tec}_cymR_P-based alginate beads after induction with cumate for 24 hours. **D)** RFU values of P_{23}_cymR-based alginate beads after induction with cumate for ~70 hours. **E**) Fold-changes (induced compared to uninduced) for the P_{23}_cymR-based beads after 70 hours of incubation. Values in the plots are the means and SD, N=3.

5) Cumate inducible system in micro-PEARLs

Encouraged by these results we proceeded to develop the PEARL system into a more compact format better suited for different applications. The PEARL format also posed other drawbacks. It is a time-consuming manual approach that can lead to fabrication errors and has poor scalability. Therefore, we adopted a more automated, time-saving, up-scalable approach to produce a higher number of beads, with smaller sizes. For that, we used the

electrospray microencapsulator B-390/B-395 (Buchi) to generate core-shell alginate micro-beads (micro-PEARLs) containing *L. plantarum* producing the red fluorescent protein, mScarlet3 intracellularly and secreting the NucA nuclease (**Figure 5A**). Hence, we could simultaneously monitor gene expression within the micro-PEARLS by tracking red fluorescence production and assess protein secretion through the DNase assay (**Figure 5B, S6A**). After incubating the micro-beads for 24 hours in a DNase plate, we could detect a prominent halo around the set of micro-PEARLs, and red fluorescence in their core. Furthermore, the halo increased in size the next day, suggesting continued secretion of NucA over time. We also incubated the micro-PEARLs in 2-mL tubes with MRS media, and the next day we could observe prominent growth within the cores even by eye (**Figure 5C**).

Next, we wanted to evaluate if these micro-PEARLs could be induced upon addition of cumate in the media. For that, we used the P_{23}_cymR variant, which would ideally produce mCherry in the core of the micro-PEARLs when cumate is added to the media (**Figure 5D**). We therefore performed the induction as in the PEARLs and after 24 hours, using fluorescence microscopy we observed mCherry expression only in the micro-PEARLs that were induced (**Figure 5E**). Furthermore, we also performed the induction of micro-PEARLs in 2-mL tubes by adding 1 mL of media with and without cumate. After 24 hours of incubation at 37 ºC, we could see remarkable differences in mCherry production for the induced and uninduced conditions (**Figure S6B**). These results validate that the more automated, time-saving, effective, and compact encapsulation method for *L. plantarum* allows the bacteria to grow efficiently while maintaining the bacteria active and responsive to the cumate inducer.

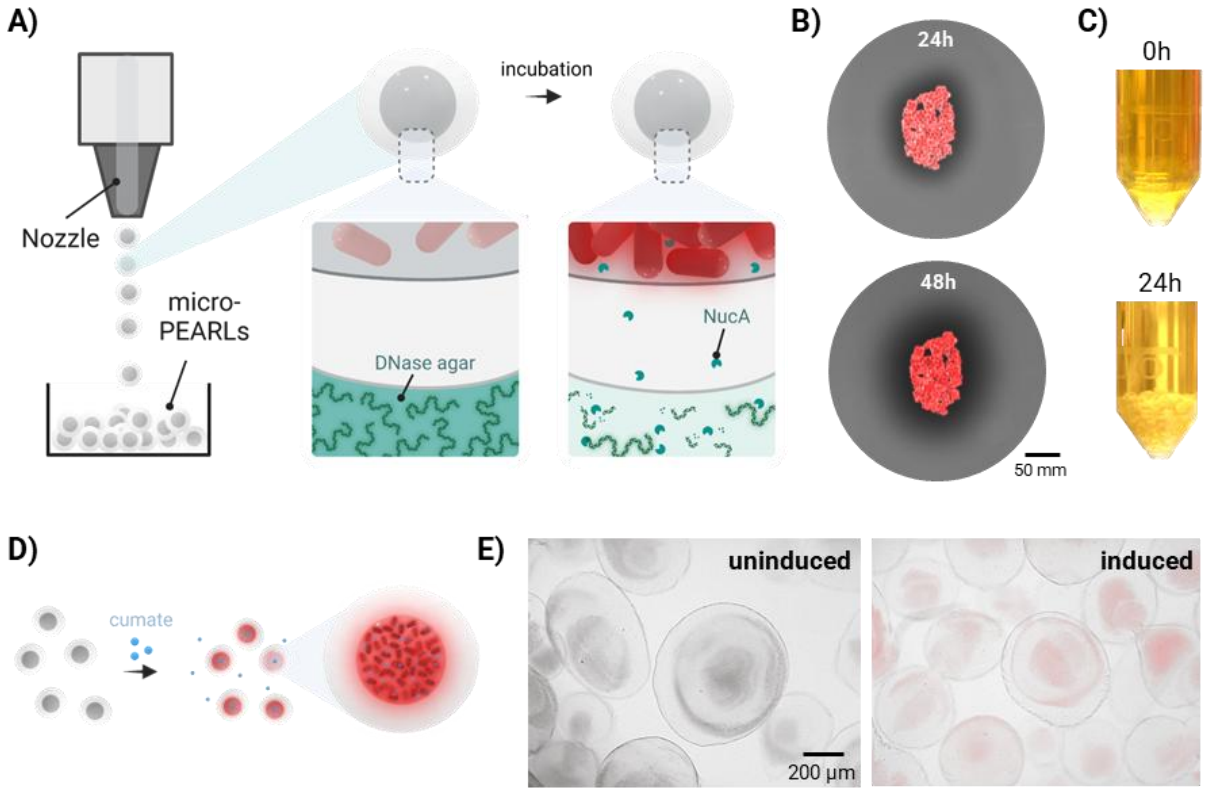

Figure 5: *Cumate inducible system in micro-PEARLs*. **A)** Scheme showing micro-PEARL fabrication with the microencapsulator. The micro-PEARLs contain bacteria that produce mScarlet3 and secretes NucA. After incubation, the core of the micro-beads turns red, and the fluorescence of the DNase agar fades away due to degradation of fluorescently labelled DNA. **B)** DNase agar plates with micro-PEARLs after 24 and 48 hours. Images taken using the BioRad Gel-Doc system. **C)** 2 mL tubes with micro-PEARLs immersed in MRS media after 0 and 24 hours. **D)** Scheme of the cumate induction in micro-PEARLs. Upon induction, the core of the beads turns red due to mCherry intracellular production. **E**) Microscopy images of uninduced and induced micro-PEARLs after 24 hours of incubation at 37 ºC.

CONCLUSIONS

In this study, we have engineered the strong constitute promoter P_{tec}, and made it responsive to cumate, thus generating a novel inducible system for *L. plantarum* WCFS1. Our results suggested that the leakiness of the cumate system is associated with bacterial growth since we consistently detected leaky expression of the inducible gene after bacteria entered the stationary phase. Nonetheless, due to the natural capacity of P_{tec} to be more active at higher temperatures, we could circumvent the leakiness of the cumate system by performing a double induction when transferring bacteria from 30ºC to 37ºC and with the addition of

cumate. Moreover, we observed the surprising effect of suppressed leaky expression in the cumate system when the engineered *L. plantarum* were encapsulated in alginate beads, as both PEARLs and micro-PEARLs formats. We hypothesize that encapsulation within alginate renders the bacteria in a prolonged pseudo-growth phase, wherein growth is severely slowed by mechanical restrictions within the material but nutrients remain available in abundance.

We believe that the cumate system can be adapted to produce other proteins of interest and become a powerful tool for engineering *L. plantarum* and related species. In addition, in combination with materials, it can advance the field of *Lactobacillus*-based ELMs and Living Therapeutic Materials.

SUPPORTING INFORMATION

Supporting information is available from the Wiley Online Library.

FUNDING

This work was supported by a Deutsche Forschungsgemeinschaft (DFG) Research grant (Project # 455063657), a DFG Collective Research Center (SFB1027) subproject grant (Project #200049484), and the Leibniz Association through the Leibniz Science Campus on Living Therapeutic Materials (LifeMat).

CONFLICT OF INTEREST

The authors declare no conflict of interest.

DATA AVAILABILITY

The raw and processed datasets along with relevant metadata are available from the corresponding author upon reasonable request.

REFERENCES

Bina, X. R., et al. (2014). "Construction of a tetracycline inducible expression vector and characterization of its use in Vibrio cholerae." Plasmid **76**: 87-94.

Blanch-Asensio, M., et al. (2023). "In vitro assembly of plasmid DNA for direct cloning in Lactiplantibacillus plantarum WCSF1." PLOS ONE **18**(2): e0281625.

Blanch-Asensio, M., et al. (2024). "Expanding the genetic programmability of Lactiplantibacillus plantarum." Microbial Biotechnology **17**(1): e14335.

Blanch-Asensio, M., et al. (2024). "Discovery of a high-performance phage-derived promoter/repressor system for probiotic lactobacillus engineering." Microbial Cell Factories **23**(1): 42.

del Rio, B., et al. (2008). "Oral Immunization with Recombinant Lactobacillus plantarum Induces a Protective Immune Response in Mice with Lyme Disease." Clinical and Vaccine Immunology **15**(9): 1429-1435.

Dey, S., et al. (2023). "Novel genetic modules encoding high-level antibiotic-free protein expression in probiotic lactobacilli." Microbial Biotechnology **16**(6): 1264-1276.

Halbmayr, E., et al. (2008). "High-Level Expression of Recombinant β-Galactosidases in Lactobacillus plantarum and Lactobacillus sakei Using a Sakacin P-Based Expression System." Journal of Agricultural and Food Chemistry **56**(12): 4710-4719.

Heiss, S., et al. (2016). "Evaluation of novel inducible promoter/repressor systems for recombinant protein expression in Lactobacillus plantarum." Microbial Cell Factories **15**(1): 50.

Karlskås, I. L., et al. (2014). "Heterologous Protein Secretion in Lactobacilli with Modified pSIP Vectors." PLOS ONE **9**(3): e91125.

Klotz, A., et al. (2023). "A Synthetic Cumate-Inducible Promoter for Graded and Homogenous Gene Expression in Pseudomonas aeruginosa." Applied and Environmental Microbiology **89**(6): e00211-00223.

Kunjapur, A. M. and K. L. J. Prather (2019). "Development of a Vanillate Biosensor for the Vanillin Biosynthesis Pathway in E. coli." ACS Synthetic Biology **8**(9): 1958-1967.

Lutz, R. and H. Bujard (1997). "Independent and Tight Regulation of Transcriptional Units in Escherichia Coli Via the LacR/O, the TetR/O and AraC/I1-I2 Regulatory Elements." Nucleic Acids Research **25**(6): 1203-1210.

Ortiz-Velez, L., et al. (2020). "Challenges and Pitfalls in the Engineering of Human Interleukin 22 (hIL-22) Secreting Lactobacillus reuteri." Frontiers in Bioengineering and Biotechnology **8**.

Pan, N., et al. (2021). "Oral Delivery of Novel Recombinant Lactobacillus Elicit High Protection against Staphylococcus aureus Pulmonary and Skin Infections." Vaccines **9**(9): 984.

Rastogi, S. and A. Singh (2022). "Gut microbiome and human health: Exploring how the probiotic genus Lactobacillus modulate immune responses." Frontiers in Pharmacology **13**.

Santos Rocha, C., et al. (2012). "Anti-inflammatory Properties of Dairy Lactobacilli." Inflammatory Bowel Diseases **18**(4): 657-666.

Scheppler, L., et al. (2002). "Recombinant Lactobacillus johnsonii as a mucosal vaccine delivery vehicle." Vaccine **20**(23): 2913-2920.

Seo, S.-O. and C. Schmidt-Dannert (2019). "Development of a synthetic cumate-inducible gene expression system for Bacillus." Applied Microbiology and Biotechnology **103**(1): 303-313.

Sørvig, E., et al. (2005). "High-level, inducible gene expression in Lactobacillus sakei and Lactobacillus plantarum using versatile expression vectors." Microbiology **151**(7): 2439-2449.

Tadimarri, V. S., et al. (2024). "PEARL: Protein Eluting Alginate with Recombinant Lactobacilli." bioRxiv: 2024.2009. 2012.612671.

Wang, J., et al. (2012). "Selection of potential probiotic lactobacilli for cholesterol-lowering properties and their effect on cholesterol metabolism in rats fed a high-lipid diet." Journal of Dairy Science **95**(4): 1645-1654.

Zhang, L., et al. (2022). "Development and Application of Two Inducible Expression Systems for Streptococcus suis." Microbiology Spectrum **10**(4): e00363-00322.